RSC Advances

PAPER

View Article Online
View Journal | View Issue

Cite this: *RSC Adv.*, 2023, **13**, 16480

Austalide derivative from marine-derived *Aspergillus* sp. and evaluation of its cytotoxic and ADME/TOPKAT properties†

Mohamed S. Elnaggar, ‡[ac] Ahmed M. Elissawy, ‡*[ab] Fadia S. Youssef, [a] Máté Kicsák,[d] Tibor Kurtán, [d] Abdel Nasser B. Singab*[ab] and Rainer Kalscheuer[c]

In-depth chemical investigation of an ethyl acetate extract of *Aspergillus* sp. isolated from the soft coral *Sinularia* species resulted in the isolation of one new meroterpenoid, austalide Z (**1**), one known austalide W (**2**), six known prenylated indole diketopiperazine alkaloids (**3–8**), and phthalic acid and its ethyl derivative (**9–10**). The structures were established by means of 1D and 2D NMR (one- and two-dimensional nuclear magnetic resonance) experiments supported by UV analysis and ESI-MS (electrospray ionization mass spectrometry). *In vitro* cytotoxic evaluation was performed against the Caco-2 cancer cell line using the MTT assay, which showed that the examined compounds had weak to moderate activities, with the new meroterpenoid austalide Z (**1**) displaying an IC_{50} value of 51.6 μg mL^{-1}. ADME/TOPKAT (absorption, distribution, metabolism, excretion, and toxicity) predication performed *in silico* showed that most of the isolated compounds possessed reasonable pharmacokinetic, pharmacodynamic, and toxicity properties. Thus, it can be concluded that *Aspergillus* sp. could act as a source of drug leads for cancer prevention with promising pharmacokinetic and pharmacodynamic properties and thus could be incorporated in pharmaceutical dosage forms.

Received 20th April 2023
Accepted 22nd May 2023

DOI: 10.1039/d3ra02632a

rsc.li/rsc-advances

1 Introduction

The fungi kingdom constitutes a rich source of bioactive compounds, and a plethora of drug candidates has been developed from fungal metabolites since the discovery of penicillin from *Penicillium notatum* by Sir Alexander Fleming in 1928. These drugs comprise the antihyperlipidemic agents atorvastatin and simvastatin, the antifungal drug griseofulvin, the anti-migraine drug ergotamine, and the immunosuppressant drug cyclosporine.[1]

Basically, endosymbiotic fungi colonize the inner tissues of a host, either plant or animal,[2] exhibiting mutual benefits, wherein the host organism provides a proper medium for the growth of the fungus and in turn the growing fungal species provide the host with bioactive compounds enabling it to survive unfavorable conditions[3] as well as mediating different ecological interactions.[4]

Endosymbiotic fungi derived from marine ecosystems have received much attention in the last two decades with the isolation of more than 1000 fungal species from marine habitats.[5] Cephalosporin C was the first bioactive molecule isolated from the marine-derived fungus *Cephalosporium* sp.,[6] and since then endosymbiotic fungi have proven to be a fabulous source of bioactive secondary metabolites belonging to different classes, such as terpenoids,[7,8] diketopiperazines,[9] polyketides,[10,11] benzophenones,[12] peptides,[13] and butyrolactones.[14]

Meroterpenoids represent a major class of fungal terpenoids,[7,15–17] and austalides represent a unique subclass of polycyclic (tetra-, penta-, hexa-, or heptacyclic) meroterpenoids with an isobenzofuranone moiety. Thus far, 38 members of austalides have been mainly isolated from different *Penicillium* and *Aspergillus* species and demonstrated potential activities, including anti-osteoporosis, antibacterial, antiviral, cytotoxic, and α-glucosidase inhibitory activities.[18–24] Moreover, many synthetic approaches have been reported for different members of the austalide family.[25–27]

It is noteworthy to highlight that cancer still represents a major impendence in the progress of therapeutic approaches to improve public health. Thus, there is an urgent search for effective naturally occurring drug candidates to combat these challenges that are less expensive and possess less adverse effects compared to the current synthetic agents.[28]

[a]*Department of Pharmacognosy, Faculty of Pharmacy, Ain Shams University Abbassia, 11566, Cairo, Egypt. E-mail: aelissawy@pharma.asu.edu.eg; dean@pharma.asu.edu.eg*

[b]*Center of Drug Discovery Research and Development, Ain Shams University Abbassia, 11566, Cairo, Egypt*

[c]*Institute of Pharmaceutical Biology and Biotechnology, Heinrich-Heine-Universität Düsseldorf, 40225, Germany*

[d]*Department of Organic Chemistry, University of Debrecen, Debrecen 4032, Hungary*

† Electronic supplementary information (ESI) available: Fig. S1–S38 comprising ^{1}H NMR, APT, 2D NMR and ESI-MS data of the isolated compounds. See DOI: https://doi.org/10.1039/d3ra02632a

‡ These authors contributed equally to the manuscript.

In continuation of our ongoing search for new secondary metabolites from marine-derived fungi, we herein report the chemical investigation of an ethyl acetate extract of the fungus *Aspergillus* sp. isolated from the inner tissues of the soft coral *Sinularia* sp. collected at the coast of Sharm El-Sheikh, Egypt. Herein, the isolation and characterization of a new meroterpenoid, named austalide Z (**1**), the known austalide W (**2**), and six known prenylated indole diketopiperazine alkaloids (**3–8**), along with phthalic acid and its ethyl derivatives (**9–10**) are reported. All the isolated compounds were assessed for their cytotoxic effect against Caco-2 cells using the MTT assay. Additionally, prediction of the pharmacokinetic and pharmacodynamic potentials as well as the toxicity properties of the isolated compounds were performed *in silico* using the ADME/TOPKAT protocol in Discovery Studio 4.5 (Accelrys Inc., San Diego, CA, USA).

2 Results and discussion

2.1. Chemical investigation of an ethyl acetate extract of the fungus *Aspergillus* sp.

In-depth chemical investigation of the ethyl acetate extract of the fungus *Aspergillus* sp. isolated from the inner tissues of the soft coral *Sinularia* sp. collected from the coast of Sharm El-Sheikh, Egypt, resulted in the isolation and characterization of one new meroterpenoid austalide Z (**1**), and one known austalide W (**2**),[19] in addition to six known prenylated indole diketopiperazine alkaloids (**3–8**),[29,30] along with phthalic acid and its ethyl derivative (**9–10**).

Compound **1** was isolated as a pale-yellow amorphous powder. LC-ESI-MS revealed pseudomolecular ion peaks at *m*/*z* 505 and 503 representing $[M + H]^+$ and $[M - H]^-$, respectively, whereas HR-ESI-MS revealed a peak at *m*/*z* 505.2068 representing $[M + H]^+$ (calculated. for *m*/*z* $C_{26}H_{33}O_{10}$, 505.2090), which corresponded to the molecular formula $C_{26}H_{32}O_{10}$ (ESI Fig. S1A & B†). The UV spectrum of **1** showed a characteristic pattern of austalides with λ_{max} at 270 nm. Its chemical structure was elucidated through 1D and 2D NMR spectroscopic analyses (ESI Fig. S2–S7†), alongside the reported data for the related analogues austalides V and W.[19] Analysis of the ^{1}H and APT-NMR spectra displayed a close similarity between compound **1** and austalide W (**2**), where the APT spectrum (Table 1) revealed the presence of 26 carbons, including one carbonyl group, six olefinic or aromatic carbons and thirteen aliphatic carbons, one tri-oxygenated quaternary carbon, one di-oxygenated quaternary carbon, three oxygenated quaternary carbons, one quaternary aliphatic carbon, one oxygenated methine carbon, one aliphatic methine carbon, two oxygenated methylene carbons, three aliphatic methylenes, two methoxyl carbons, and four methyls.

Meanwhile, the ^{1}H NMR spectrum of **1** (Table 1) displayed two methine protons at δ_H (ppm) 3.80 (1H, dd, $J = 5.5$, 0.9 Hz, H-18) and 3.05 (1H, dd, $J = 7.5$, 1.8 Hz, H-21), in which the former was oxygenated, in addition to five methylene protons at δ_H (ppm) 5.14 (2H, s, H-1), 4.16, 3.95 (2H, d, $J = 9.7$ Hz, H-25), 2.95 (2H, m, H-22), 2.64, 2.39 (2H, d, $J = 14.5$ Hz, H-12), and 2.15, 1.85 (2H, dd, $J = 15.9$, 0.9 Hz; 15.9, 5.5 Hz, H19), in which the former two methylenes were oxygenated, in addition to the presence of two methoxy protons at δ_H (ppm) 4.16 (3H, s, OMe-29) and 3.53 (3H, s, OMe-28). Moreover, four methyl protons at δ_H (ppm) 2.06 (3H, s, Me-23), 1.69 (3H, s, Me-26), 1.35 (3H, s, Me-24), and 0.87 (3H, s, Me-27) were observed.

Table 1 ^{1}H (400 MHz) and ^{13}C (100 MHz) data of compound **1** in $CDCl_3$ (δ in ppm, J in Hz)

Position	δ_C, type	δ_H (J in Hz)
1	68.2, CH_2	5.14, *s*
2		
3	169.7, C	
4	108.3, C	
5	155.3, C	
6	115.9, C	
7	157.1, C	
8	114.3, C	
9	145.5, C	
10		
11	79.2, C	
12	44.5, CH_2	2.64, d (14.5)
		2.39, d (14.5)
13	102.0, C	
14	92.2, C	
15	86.7, C	
16		
17	118.5, C	
18	69.2, CH	3.80, dd (5.5, 0.9)
19	37.7, CH_2	2.15, dd (15.9, 0.9)
		1.85, dd (15.9, 5.5)
20	39.2, C	
21	38.2, CH	3.05, dd (7.5, 1.8)
22	17.8, CH_2	2.95, m
23	10.9, CH_3	2.06, s
24	27.3, CH_3	1.35, s
25	78.2, CH_2	4.16, d (9.7)
		3.95, d (9.7)
26	23.0, CH_3	1.69, s
27	19.6, CH_3	0.87, s
28	49.1, CH_3	3.53, s
29	62.2, CH_3	4.16, s

The above-mentioned data were found to be in complete accordance with the reported data for the austalides class,[31–33] in which one known analogue of this group of compounds was also isolated here in our study from the same crude extract, namely austalide W (**2**).[31] Compound **2** was found to exhibit close similarity to the structure of **1**. Moreover, it is worthy to highlight that **2** was previously reported to be the first austalide derivative having a 5/6/6/6/6/5/5 heptacyclic ring system, including a tetrahydrofuranyl ring.[31] In addition, this ring system was also confirmed in **1** to be in alignment with all previously reported austalides, as well as the affirmation of the presence of ring G through the existence of the down-fielded CH_2 group (C-25) at δ_H (ppm) 4.16, 3.95 (2H, d, $J = 9.7$ Hz) and δ_C (ppm) 78.2, alongside the existence of a characteristic down-field carbon shift of C-13 at δ_C (ppm) 102.0, in which all those characteristic shifts were found to be similar to **2**,[31] affirming the presence of the unusual tetrahydrofuranyl ring (ring G) in the structure of **1**.

By inspection of the NMR data mentioned above for **1**, it was clear that it differed from austalide W (**2**) only by the presence of a newly added hydroxyl group at C-18. This hydroxylation could be unambiguously deduced through the difference of the molecular weight of both compounds by only 16 units in the molecular weight of **1** compared to **2**. Moreover, in the COSY spectrum, there was a distinct correlation between H-18 and H_2-19, confirming the adjacent positioning of both groups. This suggestion was further confirmed through inspection of the reported data for **2** in comparison to the data of the newly isolated **1**, in which instead of the methylene group at C-18 in **2**, a clearly observed oxygenated methine proton was detected at δ_H (ppm) 3.8 on C-18. Hence, there was a low-field chemical shift from δ_H (ppm) 1.81–1.94 in **2** (ref. 31) to δ_H (ppm) 3.8 in **1**, as well as a low-field shift of carbon from δ_C (ppm) 30.92 in **2** (ref. 31) to δ_C (ppm) 69.2 in **1**. In addition, a low-field shift was also detected in APT NMR for C-19 from δ_C (ppm) 30.83 in **2** (ref. 31) to δ_C (ppm) 37.7 in **2**, side by side with the confirmatory HMBC correlations from the newly observed methine proton H-18 to δ_C 39.2 (C-20) and δ_C 118.5 (C-17), as well as with the correlations from δ_H (ppm) 0.87 (H_3-27) and δ_H (ppm) 2.15, 1.85 (H_2-19) toward δ_C (ppm) 69.2 (C-18). It is noteworthy to mention that Antipova *et al.* isolated an acetylated derivative, austalide V, where the oxygenated methine was placed at C-19.[34] In our case, HMBC correlations confirmed the presence of the oxygenated methine at C-18 instead, as revealed by the absence of strong correlations between the methyl protons of C-27 and the oxygenated methine carbon C-18. Thus, **1** possessed a heptacyclic skeleton the same as other austalide analogues and the planar structure was elucidated as shown. The trivial name austalide Z is proposed.

The relative configuration of the eight chirality centers of **1** was determined based on NOESY correlations (Fig. 2). A NOESY correlation between 26-H and 27-H methyl protons suggested the *cis* diaxial orientation of the two methyl groups and determined the relative configuration of the C-14 and C-17 bridge-head carbons, similarly to other previously reported austalide analogues.[31] Moreover, the NOE correlations of 24-H methyl protons with the 21-H methine proton indicated that the C-11 and C-21 bridge-head carbons had *cis* relative configurations. In addition, the observed NOE correlations between the oxygenated 18-H methine proton with the 21-H methine proton

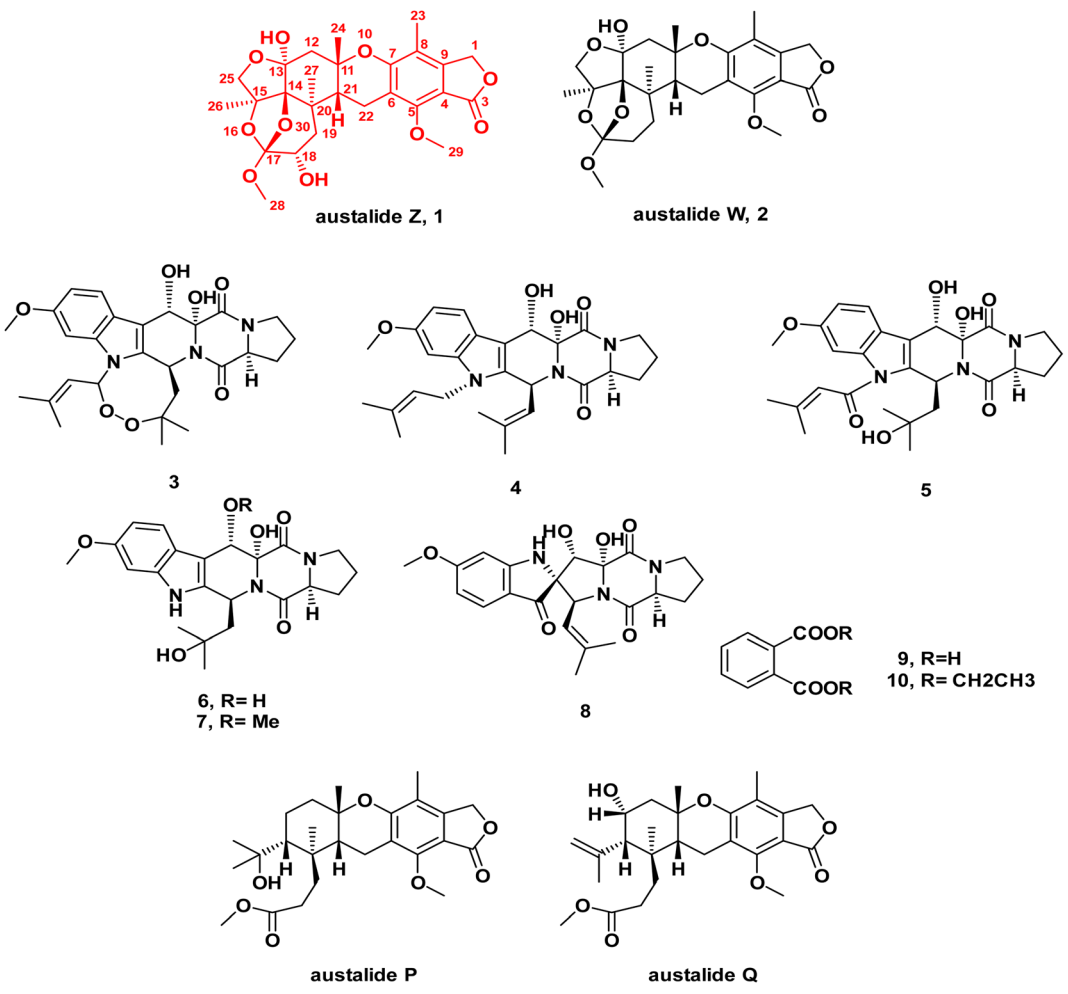

Fig. 1 Chemical structures of compounds **1–10** isolated from the ethyl acetate extract of the fungus *Aspergillus* sp. obtained from the soft coral *Sinularia* sp.

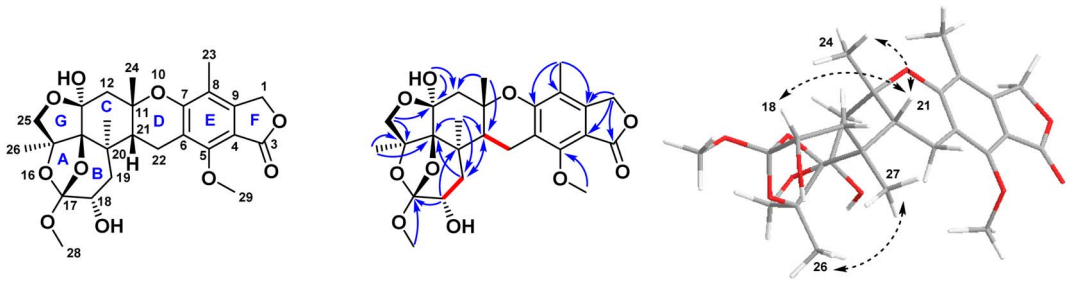

Fig. 2 Key COSY, HMBC, and NOESY correlations of compound **1** isolated from the ethyl acetate extract of the fungus *Aspergillus* sp. obtained from the soft coral *Sinularia* sp.

alongside with the absence of any cross-peaks or correlations of the former proton with either C-26 or C-27, revealed the *cis* orientations of 21-H and 18-H. Thus, the relative configuration of **1** was determined as (11*S**, 13*S**, 14*S**,15*S**,17*S**,18*S**,20*R**,21*R**).

In addition, the biosynthesis of all austalide derivatives likely followed the same biosynthetic pathway, suggesting that they all originated from the parent 6-[(2*E*,6*E*)-farnesyl]-5,7-dihydroxy-4-methylphthalide followed by cyclization and oxidative modification.[31] An additional pathway for austalide derivatives was proposed based on the reported total synthesis of austalide B.[35,36] Thus, those two reported biosynthetic pathways suggested that the skeleton had the same configuration for all the austalide group members.

The ECD spectrum of austalide Z (Fig. 3) showed negative cotton effects (CEs) at 266 and 213 nm and a positive one at 229 nm, which were quite similar to those of the tetracyclic austalides P and Q (Fig. 1).[23] The absolute configuration of austalide P was previously determined by one of the authors,[23] using the solution TDDFT-ECD calculation protocol.[37] In the absence of the C-22 benzylic chirality center, the ECD spectra of austalides Z, P, and Q are governed by the absolute configuration of the C-11 and C-21 bridge-head chirality centers, which have the same (11*S*,21*R*) absolute configuration. Moreover, the ECD spectrum of austalide Z showed a similar pattern to those of austalides V and W. With knowledge of the (11*S**,13*S**,14*S**,15*S**,17*S**,18*S**,20*R**,21*R**) relative configuration, the ECD pattern of austalide Z was derived from the (11*S*,13*S*,14*S*,15*S*,17*S*,18*S*,20*R*,21*R*) absolute configuration.

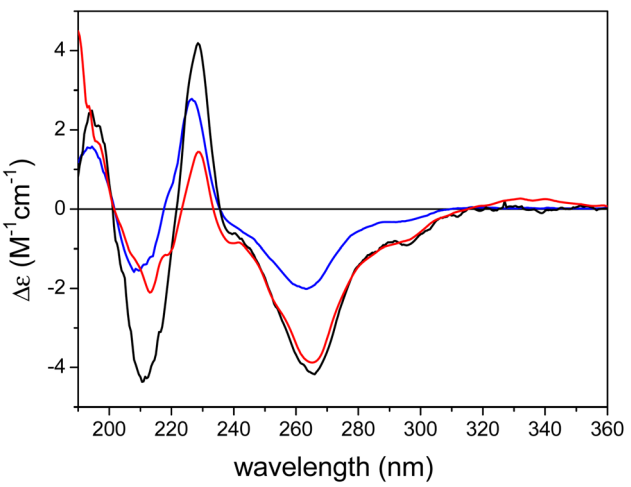

Fig. 3 Experimental ECD spectra of austalide Q (X, blue), austalide P (Y, black) *versus* austalide Z (**1**, red) in acetonitrile; Copyright Wiley-VCH GmbH. Reproduced with permission. Y. Zhou, A. Mándi, A. Debbab, V. Wray, B. Schulz, W. E. Müller, W. Lin, P. Proksch, T. Kurtán, A. H. Aly, New Austalides from the Sponge-Associated Fungus *Aspergillus* sp., *Eur. J. Org. Chem.*, 2011 (**2011**) 6009.[23]

2.2. *In vitro* cytotoxic evaluation of the isolated compounds using the MTT assay

Cytotoxic evaluations of **3**, **4**, **6**, **8** (diketopiperazine derivatives) as well as **1** and **2** (meroterpenoid derivatives) against Caco-2 (human colorectal carcinoma cell lines) revealed weak to moderate activities, displaying IC_{50} values ranging between 32.5 and 126 μg mL^{-1}, where the new meroterpenoid austalide Z (**1**) displayed a cytotoxic effect, with an IC_{50} of 51.6 μg mL^{-1}, as illustrated in Table 2.

2.3. ADME/TOPKAT prediction

Prediction of the pharmacokinetic and pharmacodynamic potential as well as the toxicity properties of the isolated compounds was performed *in silico* using the ADME/TOPKAT protocol in Discovery Studio 4.5 (Accelrys Inc., San Diego, CA, USA). Regarding human intestinal descriptor, **1**, **2**, **4**, and **7–10** showed good human intestinal absorption levels and thus lay within the 99% absorption ellipse as displayed in the ADMET

Table 2 Cytotoxic activity (IC_{50} μg mL^{-1}) of compounds isolated from the ethyl acetate extract of the fungus *Aspergillus* sp. obtained from the soft coral *Sinularia* sp. against the Caco-2 cancer cell line

Compound	IC_{50} μg mL^{-1}
1	51.6 ± 0.88
2	57.0 ± 0.45
3	126.0 ± 0.90
4	32.5 ± 0.73
6	105.0 ± 0.54
8	51.9 ± 0.35
Doxorubicin[a]	1.25 ± 0.22

[a] Positive control.

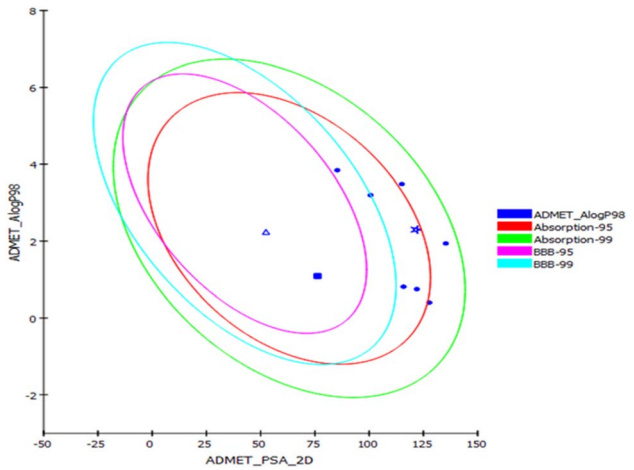

Fig. 4 ADMET plot for compounds identified from *Aspergillus* sp. displaying the 95% and 99% confidence limit ellipses corresponding to the blood–brain barrier (BBB) and the human intestinal absorption. Austalide Z (**1**) (star); compound **9** (triangle); compound **10** (filled square).

plot (Fig. 4). Concerning the solubility level, **10** showed optimal solubility, while the rest of the compounds revealed possible or good solubility levels. Also, **4**, **9**, and **10** revealed medium to low blood–brain barrier (BBB) penetration levels and thus lay inside the 99% BBB confidence eclipse in the ADMET plot (Fig. 4). On the contrary, the rest of the compounds had undefined BBB penetration levels, taking level 4 and thus lay outside the 99% BBB confidence eclipse. Regarding the binding of the compounds with plasma protein, **3–8** and **10** displayed less than 90% plasma protein binding (PPB), while the rest of the compounds showed more than 90% PPB. Additionally, all the isolated compounds showed no inhibition to CYP2D6, but some of the compounds showed certain hepatotoxic effects, such as **3–8** and **10** (Table 3).

Regarding TOPKAT prediction, all the examined isolated compounds displayed no mutagenicity as predicted by the chemical Ames mutagenicity protocol done *in silico*. Furthermore, **3–5** and **7** showed no carcinogenic effect to both male and female rats (NTP), whereas **9–10** exhibited some carcinogenic potential for female rats and **1–2** and **6–8** for male rats. They displayed rat oral LD50 values between 0.16–9.68 g kg^{-1}-body-weight, with **9–10** showing the highest LD50s of 9.68 and 4.05 g kg^{-1}-body-weight, respectively. Similarly for the rat chronic LOAEL level, all the isolated compounds displayed values between 0.0017–1.6549 g kg^{-1}-body-weight, with **9–10** showing the highest LOAELs of 0.9889 and 1.6549 g kg^{-1}-body-weight, respectively. Regarding skin irritancy, most of the isolated compounds showed no to mild skin irritation. For ocular irritation, most of the isolated compounds showed no to mild irritation except for **6–8** and **10**, which showed moderate eye irritation. Thus, it can be concluded that most of the isolated compounds showed reasonable *in silico* pharmacokinetic, pharmacodynamic, and toxicity properties, and thus could potentially be incorporated in pharmaceutical dosage forms to prevent cancer. Additionally, **9** and **10** that showed the highest fitting scores revealed the best pharmacokinetic and pharmacodynamic properties with slight toxicity, which could be controlled by the given doses when formulated in pharmaceutical preparations (Table 4).

3 Experimental section

3.1. General experimental procedures

NMR spectra (chemical shifts in ppm) were recorded on a Bruker AVANCE HD III 400 MHz spectrometer (Switzerland). NMR samples were dissolved in methanol-d_4 or chloroform-d_3, (Sigma Aldrich, Germany) and transferred to 3 mm NMR tubes (Bruker). ECD spectra were recorded on a J-810 spectropolarimeter. HR-ESI-MS analyses were performed on an FTHRMS-Orbitrap (Thermo Finnigan) mass spectrometer. LC-PDA-MS analyses were performed using a Shimadzu LCMS 8045 system coupled with a photodiode array detector (LC-2030/2040) with detection wavelengths of 235, 254, and 280 nm with λ_{max} absorption at 220–400 nm. The LC-PDA-MS system was equipped with an RP-C18 UPLC column (shimpack 2 mm × 150

Table 3 Absorption, distribution, metabolism, excretion, and toxicity (ADMET) predictions of compounds (**1–10**) isolated from the ethyl acetate extract of *Aspergillus* sp. obtained from the soft coral *Sinularia* species[a]

Compound	Absorption level	Solubility level	BBB level	PPB level	CPY2D6	Hepatotoxic	PSA-2D	Alog p98
1	0	2	4	True	NI	NT	2.30	121.44
2	0	1	3	True	NI	NT	3.20	100.63
3	1	2	4	False	NI	Tox	3.49	115.08
4	0	2	2	False	NI	Tox	3.84	85.33
5	1	3	4	False	NI	Tox	1.94	135.33
6	1	3	4	False	NI	Tox	0.40	127.74
7	0	3	4	False	NI	Tox	0.81	115.85
8	0	3	4	False	NI	Tox	0.75	121.98
9	0	3	2	True	NI	NT	2.24	52.46
10	0	4	3	False	NI	Tox	1.09	76.23

[a] 0, 1, 2, and 3 indicates good, moderate, low, and very low absorption, respectively; 0, 1, 2, 3, 4, and 5 indicates extremely low, very low but possible, low, good, optimal, and too soluble, respectively; 0, 1, 2, 3, and 4 denote very high, high, medium, low, and undefined, penetration *via* BBB respectively. PBB, plasma protein binding, FALSE means less than 90%, TRUE means more than 90%. NI: non-inhibitor. NT: non-toxic; Tox., toxic. PSA 2D: 2D polar surface area. Alog P98: logarithm of the partition coefficient between *n*-octanol and water.

Table 4 TOPKAT (toxicity prediction) analysis of compounds (**1–10**) isolated from the ethyl acetate extract of *Aspergillus* sp. obtained from the soft coral *Sinularia* species[a]

Compounds	Ames prediction	Rat oral LD50	Rat chronic LOAEL	Skin irritancy	Ocular irritancy	Rat female NTP	Rat male NTP
1	Non-mutagen	0.16	0.0038	Mild	None	Non-carcinogen	Carcinogen
2	Non-mutagen	0.29	0.0033	Mild	None	Non-carcinogen	Carcinogen
3	Non-mutagen	1.14	0.0043	Mild	Mild	Non-carcinogen	Non-carcinogen
4	Non-mutagen	1.43	0.0026	Mild	Mild	Non-carcinogen	Non-carcinogen
5	Non-mutagen	1.34	0.0036	Mild	Mild	Non-carcinogen	Non-carcinogen
6	Non-mutagen	0.82	0.0145	None	Moderate	Non-carcinogen	Carcinogen
7	Non-mutagen	0.89	0.0076	Mild	Moderate	Non-carcinogen	Carcinogen
8	Non-mutagen	0.56	0.0218	None	Moderate	Non-carcinogen	Carcinogen
9	Non-mutagen	9.68	0.9891	Mild	None	Carcinogen	Non-carcinogen
10	Non-mutagen	4.05	1.6549	None	Moderate	Carcinogen	Non-carcinogen

[a] Both rat oral LD5 and rat chronic LOAEL are expressed in g kg^{-1}-body-weight.

mm) possessing 2.7 μm particle size using the following gradient elution (acetonitrile (ACN), 0.1% HCOOH in H_2O) 0–2 min (10% MeOH); 2–35 min (10% ACN-100% ACN), and 35–40 (100% ACN) with a 0.2 mL min^{-1} flow rate. The final purification steps were performed using preparative HPLC (Shimadzu, Japan) using a Kromasil C-18RP semi-preparative column (10 mm × 250 mm) at a flow rate of 5 mL min^{-1} and UV detection at wavelength of 254 nm with a λ_{max} absorption at 220–400 nm. Medium pressure liquid chromatography was performed on a Puriflash 4125 system equipped with a PDA detector. Normal phase column chromatography was performed using silica gel 60 (0.04–0.063, Merck, Germany). TLC analyses were performed using normal phase silica gel precoated plates F_{254} (Merck, Germany). All the consumed solvents were of analytical grade, while those used for HPLC analyses were of HPLC grade.

3.2. Fungal material

The fungus *Aspergillus* sp. was isolated from the inner tissues of the marine soft coral *Sinularia* sp. The soft coral was collected from the Red Sea close to Sharm El-Sheikh, Egypt, in September 2018 at 5–7 meters depth. For isolation of the fungal strain, the soft coral was rinsed with distilled water, and then surface sterilization was performed using 70% ethanol for 2 min. Small samples from the inner tissues of the soft coral were aseptically cut using a sterilized blade and pressed onto malt agar plate (15 g L^{-1} malt extract, 15 g L^{-1} agar, 0.2 g L^{-1} chloramphenicol to suppress bacterial growth, with the pH adjusted to 7.4–7.8 using 10% NaOH). After incubation at 25 °C, the fungal strain under investigation was found to grow out of the sponge tissue. Pure fungal strains were grown by repeated re-inoculation on fresh culture media.

3.3. Identification of the fungal strain

The isolated fungal strain was identified as *Aspergillus* sp. using a molecular biological protocol by DNA amplification and by sequencing of the ITS region as previously reported.[38] The obtained data of sequencing were submitted to GenBank with the accession number OK035701.

3.4. Cultivation, extraction, and isolation

Small scale fermentation of the fungal strain was performed on solid rice culture media (100 g rice in 110 mL distilled water, autoclaved for 20 min at 121 °C) in a 1 L Erlenmeyer flask (2 flasks were used). The culture was incubated for 30 days at 25 °C under static conditions. Large-scale fermentation was performed on solid rice medium using 12 Erlenmeyer flasks (1 L each). Fungal cultures were extracted using ethyl acetate (EtOAc), and the combined extracts were then evaporated in vacuum and the residue was partitioned between *n*-hexane and 90% aqueous methanol yielding about 3 g of reddish-brown solid residue.

The defatted extract was then applied to vacuum liquid chromatography (VLC) packed with normal phase silica gel as the stationary phase and applying a stepwise gradient as follows: 80% *n*-hexane in ethyl acetate to 100% ethyl acetate, followed by dichloromethane in methanol from 95% to 50%. Eluted fractions were analyzed using TLC and similar fractions were pooled together yielding 7 major fractions (FR1–7). Fraction FR3 (500 mg) was fractionated using normal phase medium pressure liquid chromatography eluted with a linear gradient elution from 80% *n*-hexane: EtOAc to 30% *n*-hexane: EtOAc. Final purification was performed using RP-semi-preparative HPLC, eluted with a linear gradient elution from 70% ACN : H_2O to 95% ACN : H_2O with the final purification of two compounds **3** (25 mg) and **4** (30 mg). Fraction FR4 (350 mg) was directly applied to semi-preparative HPLC and subsequently eluted with a linear gradient elution from 50% ACN : H_2O to 90% ACN : H_2O yielding **1** (9 mg), **5** (15 mg), and **10** (30 mg). Fraction FR5 (700 mg) was fractionated using normal phase medium pressure liquid chromatography (Puriflash®) eluted with a linear gradient elution from dichloromethane: methanol gradient (from 100% to 80%) yielding three major sub-fractions FR5-V1–FR5-V3. Fraction FR5-V1 was purified using RP-semi-prep-HPLC-PDA eluted with a linear gradient elution from 20% ACN : H_2O to 60% ACN : H_2O yielding **2** (12 mg) and **9** (20 mg). Similarly, fraction FR5-V3 was purified using semi-prep HPLC and eluted using 30% ACN : H_2O to 60% ACN : H_2O yielding **6** (11 mg), **7** (7 mg), and **8** (4 mg).

3.5. Compound characterization

Austalide Z (**1**): pale-yellow amorphous powder. ^{1}H (400 MHz) and ^{13}C (100 MHz) data in $CDCl_3$, as illustrated in Table 1. ECD: ($c = 5.5 \times 10^{-5}$ M, MeCN) λ [nm], ($\Delta\varepsilon$) = 332 (0.26), 296sh (−0.79), 266 (−3.88), 240sh (−0.87), 229 (1.45), 219sh (−1.16), 213 (−2.11); $[\alpha]_D^{20}$ = (c 0.10, $CDCl_3$); LC-ESI-MS revealed a pseudomolecular ion peak at m/z 505 and 503 $[M + H]^+$ and $[M - H]^-$, respectively, whereas HR-ESI-MS $[M + H]^+$ showed a peak at m/z 505.2068 (calculated. for m/z $C_{26}H_{33}O_{10}$, 505.2090) corresponding to the molecular formula $C_{26}H_{32}O_{10}$. Different spectra are available in the ESI (Fig. S1†).

3.6. Cytotoxicity assay

MTT assay was carried out as previously described[39] with some modifications. Basically, 100 μL of the tested compound was dissolved in 5% DMSO and RPMI (Roswell Park Memorial Institute) tissue culture medium was then added to each well to reach a final concentration of X μg mL^{-1}. Control wells contained two aliquots of 100 μL of tissue culture medium (MEM + fetal bovine serum in a ratio 9 : 1), 100 μL sterile DMSO (5%), and RPMI tissue culture medium. Following the specified incubation period (24 h) at 37 °C, the wells were washed with PBS (phosphate Buffered Saline) and the cells were incubated with MTT solution (2 mg mL^{-1}) at 100 μL per each well for 1 h at 37 °C. The supernatants were then removed by decantation and the cells were treated with 100 μL of DMSO per each well to dissolve the formazan crystals formed in the viable metabolically active cells. Elutes of the 8 wells of each test isolate were collected and the absorbance was measured at 540 nm. Control wells were similarly treated and the percentage cytotoxicity was calculated employing the following formula;[39,40] cytotoxicity% = 1 − {A_{540} of test culture/A_{540} of control culture} × 100.

3.7. ADME/TOPKAT prediction

ADME/TOPKAT (absorption, distribution, metabolism, excretion, and toxicity) prediction was performed for the isolates using Discovery Studio 4.5 (Accelrys Inc., San Diego, CA, USA). The aqueous solubility, plasma protein binding prediction (PPB), human intestinal absorption, blood–brain barrier penetration (BBB), cytochrome P450 (2D6), and hepatotoxicity level were chosen as the ADME descriptors. Meanwhile, the carcinogenic effect on male and female rat FDA, ocular and skin irritation, rat oral LD50, Ames mutagenicity, and rat chronic LOAEL were selected as the toxicity parameters.[41,42]

4 Conclusions

In-depth chemical investigation of the ethyl acetate extract of marine fungus *Aspergillus* sp. isolated from the inner tissues of the soft coral *Sinularia* sp. resulted in the isolation of one new meroterpenoid austalide Z in addition to nine known compounds belonging to the austalide class, prenylated indole diketopiperazine alkaloids, and phthalic acid derivatives. *In vitro* cytotoxic evaluation using the MTT assay revealed that most of the examined compounds showed weak to moderate activities, with austalide Z displaying substantial cytotoxic activity. ADME/TOPKAT showed that most of the isolated compounds displayed reasonable pharmacokinetic, pharmacodynamic, and toxicity properties. Thus, it can be concluded that *Aspergillus* sp. could act as a source of drug leads that could alleviate cancer with reasonable pharmacokinetic and pharmacodynamic properties that could be further improved *via* various treatments and hence could be incorporated in pharmaceutical dosage forms. However, additional *in vivo* studies followed by preclinical trials are highly recommended to be conducted on the isolated compounds to confirm the obtained results.

Author contributions

Conceptualization, A. S and M. E.; methodology, A. E, M. E., T. K., M. K.; software, F. Y.; validation, R. K., A. S and T. K.; investigation, A. E.; F. S., M. E., M. K. and T. K.; resources, A. S and R. K.; writing—original draft preparation, M. E., A. E., F. Y. And M. K.; writing—review and editing, A. S., T. K., R. K.; supervision, A. S. and R. K.; project administration, A. E. funding acquisition, A. S. and R. K. All authors have read and agreed to the published version of the manuscript.

Conflicts of interest

There are no conflicts to declare.

Acknowledgements

The research work of M. E, A. E and A. S. was funded by The Science, Technology, and Innovation Funding Authority; STIFA through Joint Egyptian Japanese Scientific Cooperation (JEJSC) grant no. 28925 entitled “Chemical biology on innovative biologically active metabolites from endosymbionts in Egyptian marine invertebrates”. The research work of T. K. and M. K. was supported by the National Research, Development and Innovation Office (K138672). M. S. Elnaggar thanks the Ministry of Higher Education of the Arab Republic of Egypt for fully funding postdoctoral mission. The authors would like thank the CeMSA@HHU (Center for Molecular and Structural Analytics @ Heinrich Heine University) for recording the mass-spectrometric and the NMR spectroscopic data.

Notes and references

1 N. G. Gomes, F. Lefranc, A. Kijjoa and R. Kiss, *Mar. Drugs*, 2015, **13**, 3950–3991.
2 R. X. Tan and W. X. Zou, *Nat. Prod. Rep.*, 2001, **18**, 448–459.
3 M. C. Leal, C. Sheridan, R. Osinga, G. Dionísio, R. J. M. Rocha, B. Silva, R. Rosa and R. Calado, *Mar. Drugs*, 2014, **12**, 3929–3952.
4 V. J. Paul and M. P. Puglisi, *Nat. Prod. Rep.*, 2004, **21**, 189–209.
5 J. F. Imhoff, *Mar. Drugs*, 2016, **14**, 19.
6 J. Silber, A. Kramer, A. Labes and D. Tasdemir, *Mar. Drugs*, 2016, **14**, 137.
7 A. M. Elissawy, M. El-Shazly, S. S. Ebada, A. B. Singab and P. Proksch, *Mar. Drugs*, 2015, **13**, 1966–1992.

8 M. S. Elnaggar, S. S. Ebada, M. L. Ashour, W. Ebrahim, A. Singab, W. Lin, Z. Liu and P. Proksch, *Fitoterapia*, 2017, **116**, 126–130.
9 A. M. Elissawy, S. S. Ebada, M. L. Ashour, M. El-Neketi, W. Ebrahim and A. B. Singab, *Phytochem. Lett.*, 2019, **29**, 1–5.
10 M. S. Elnaggar, S. S. Ebada, M. L. Ashour, W. Ebrahim, W. E. Müller, A. Mándi, T. Kurtán, A. Singab, W. Lin and Z. Liu, *Tetrahedron*, 2016, **72**, 2411–2419.
11 M. S. Elnaggar, W. Ebrahim, A. Mándi, T. Kurtán, W. E. G. Müller, R. Kalscheuer, A. Singab, W. Lin, Z. Liu and P. Proksch, *RSC Adv.*, 2017, **7**, 30640–30649.
12 M. Bai, C. H. Gao, K. Liu, L. Y. Zhao, Z. Z. Tang and Y. H. Liu, *J. Antibiot.*, 2021, **74**, 821–824.
13 F. S. Youssef, M. L. Ashour, A. N. B. Singab and M. Wink, *Mar. Drugs*, 2019, **17**, 559.
14 R. Zhang, W. He, Y. Wang, J. Zhao, R. Zhou, L. Li, Y. He, S. Cen and L. Yu, *J. Antibiot.*, 2021, **74**, 225–232.
15 A. M. Elissawy, S. S. Ebada, M. L. Ashour, F. C. Özkaya, W. Ebrahim, A. B. Singab and P. Proksch, *Phytochem. Lett.*, 2017, **20**, 246–251.
16 Y. Matsuda and I. Abe, *Nat. Prod. Rep.*, 2016, **33**, 26–53.
17 B. Sontag, N. Arnold, W. Steglich and T. Anke, *J. Nat. Prod.*, 1999, **62**, 1425–1426.
18 l. liu and h. ruan, *Phytochem. Lett.*, 2022, **47**, 12.
19 T. V. Antipova, K. V. Zaitsev, Y. F. Oprunenko, A. Y. Zherebker, G. K. Rystsov, M. Y. Zemskova, V. P. Zhelifonova, N. E. Ivanushkina and A. G. Kozlovsky, *Bioorg. Med. Chem. Lett.*, 2019, **29**, 6.
20 K. J. Kim, J. Lee, W. Wang, Y. Lee, E. Oh, K. H. Park, C. Park, G. E. Woo, Y. J. Son and H. Kang, *Int. J. Mol. Sci.*, 2021, **22**, 12.
21 J. X. Peng, X. M. Zhang, W. Wang, T. J. Zhu, Q. Q. Gu and D. H. Li, *Mar. Drugs*, 2016, **14**, 9.
22 J. Wang, Y. N. Sang, S. Q. Tang and P. Zhang, *Chem. Nat. Compd.*, 2020, **56**, 670–673.
23 Y. Zhou, A. Mándi, A. Debbab, V. Wray, B. Schulz, W. E. Müller, W. Lin, P. Proksch, T. Kurtán and A. H. Aly, *Eur. J. Org. Chem.*, 2011, **2011**, 6009.
24 A. E. Dejesus, R. M. Horak, P. S. Steyn and R. Vleggaar, *J. Chem. Soc., Chem. Commun.*, 1983, 716–718, DOI: **10.1039/c39830000716**.
25 T. K. Ma, P. J. Parsons and A. G. M. Barrett, *J. Org. Chem.*, 2019, **84**, 4961–4970.
26 L. A. Paquette and M. M. Schulze, *Heterocycles*, 1993, **35**, 585–589.
27 L. A. Paquette, T. Z. Wang and M. R. Sivik, *J. Am. Chem. Soc.*, 1994, **116**, 2665–2666.
28 F. S. Youssef, E. Alshammari and M. L. Ashour, *Int. J. Mol. Sci.*, 2021, **22**, 1866.
29 F. Wang, Y. Fang, T. Zhu, M. Zhang, A. Lin, Q. Gu and W. Zhu, *Tetrahedron*, 2008, **64**, 7986–7991.
30 F. Xie, X. B. Li, J. C. Zhou, Q. Q. Xu, X. N. Wang, H. Q. Yuan and H. X. Lou, *Chem. Biodiversity*, 2015, **12**, 1313–1321.
31 T. V. Antipova, K. V. Zaitsev, Y. F. Oprunenko, A. Ya. Zherebker, G. K. Rystsov, M. Y. Zemskova, V. P. Zhelifonova, N. E. Ivanushkina and A. G. Kozlovsky, *Bioorg. Med. Chem. Lett.*, 2019, **29**, 126708.
32 J. Peng, X. Zhang, W. Wang, T. Zhu, Q. Gu and D. Li, *Mar. Drugs*, 2016, **14**, 131.
33 Y. Zhou, A. Debbab, V. Wray, W. Lin, B. Schulz, R. Trepos, C. Pile, C. Hellio, P. Proksch and A. H. Aly, *Tetrahedron Lett.*, 2014, **55**, 2789–2792.
34 T. V. Antipova, K. V. Zaitsev, Y. F. Oprunenko, A. Y. Zherebker, G. K. Rystsov, M. Y. Zemskova, V. P. Zhelifonova, N. E. Ivanushkina and A. G. Kozlovsky, *Bioorg. Med. Chem. Lett.*, 2019, **29**, 126708.
35 L. A. Paquette, T.-Z. Wang and M. R. Sivik, *J. Am. Chem. Soc.*, 1994, **116**, 2665–2666.
36 L. A. Paquette, T.-Z. Wang and M. R. Sivik, *J. Am. Chem. Soc.*, 1994, **116**, 11323–11334.
37 A. Mándi and T. Kurtán, *Nat. Prod. Rep.*, 2019, **36**, 889–918.
38 J. Kjer, A. Debbab, A. H. Aly and P. Proksch, *Nat. Protoc.*, 2010, **5**, 479–490.
39 A. M. Saliba, A. Filloux, G. Ball, A. S. Silva, M.-C. Assis and M.-C. Plotkowski, *Microb. Pathog.*, 2002, **33**, 153–166.
40 J. Murakami, K. Kishi, K. Hirai, K. Hiramatsu, T. Yamasaki and M. Nasu, *Int. J. Antimicrob. Agents*, 2000, **15**, 103–109.
41 A. Mollica, G. Zengin, S. Durdagi, R. Ekhteiari Salmas, G. Macedonio, A. Stefanucci, M. P. Dimmito and E. Novellino, *J. Biomol. Struct. Dyn.*, 2019, **37**, 726–740.
42 F. S. Youssef, E. Ovidi, N. M. A. Musayeib and M. L. Ashour, *Plants*, 2021, **10**, 1953.